Journal of *Fungi*

MDPI

Article

Novel Metabolites of *Xylaria thienhirunae* SWUF17-44.1 with Biological Activities and Molecular Docking Analysis

Pitchapa Thongsuwan [1], Lutfun Nahar [2], Satyajit D. Sarker [2], Pitchaya Kongmaung [1], Kiattawee Choowongkomon [3,4], Cherdchai Phosri [5] and Nuttika Suwannasai [1,*]

[1] Department of Microbiology, Faculty of Science, Srinakharinwirot University, 114 Sukhumvit 23, Wattana, Bangkok 10110, Thailand; pitchapa.jang@g.swu.ac.th (P.T.); pitchaya.kong@g.swu.ac.th (P.K.)
[2] Centre for Natural Products Discovery, School of Pharmacy and Biomolecular Sciences, Liverpool John Moores University, Byrom Street, Liverpool L3 3AF, UK; l.nahar@ljmu.ac.uk (L.N.); s.sarker@ljmu.ac.uk (S.D.S.)
[3] Department of Biochemistry, Faculty of Science, Kasetsart University, Bangkok 10900, Thailand; kiattawee.c@ku.ac.th
[4] Center for Advanced Studies in Nanotechnology for Chemical, Food and Agricultural Industries, KU Institute for Advanced Studies, Kasetsart University, Bangkok 10900, Thailand
[5] Department of Biology, Faculty of Science, Nakhon Phanom University, Nakhon Phanom 48000, Thailand; cherd.phosri@npu.ac.th
* Correspondence: nuttika@g.swu.ac.th; Tel.: +66-8-67239088

Abstract

The extract of *Xylaria thienhirunae* SWUF17-44.1 displayed broad-spectrum antimicrobial activity, with higher potency against Gram-positive bacteria than Gram-negative strains. Minimum inhibitory concentration (MIC) values were as low as 0.63 μg/μL for *Staphylococcus aureus* and 1.25 μg/μL for *Bacillus subtilis*, whereas higher values were observed for *Escherichia coli* and *Pseudomonas aeruginosa*. The extract also inhibited fungal growth, with MICs of 6.25 μg/μL against *Candida albicans* and *C. tropicalis*. Strong antioxidant activity was observed (DPPH IC_{50} = 0.706 ± 0.022 μg/μL; ABTS IC_{50} = 0.251 ± 0.019 μg/μL), correlated with high phenolic content. Moderate anti-inflammatory activity was confirmed via nitric oxide inhibition. LC-MS profiling indicated diverse metabolites, including phenolic derivatives, aminoglycoside-like compounds, and annotated bioactive molecules. Chromatographic isolation yielded four compounds: 4-(2,3-dihydroxypropoxy)benzoic acid, 4-prenyloxybenzoic acid, and two novel metabolites, xylerithienol and xylerithiether. In silico docking predicted strong interactions of the novel compounds with bacterial targets such as muramyl ligases, DNA gyrase B, and β-ketoacyl-ACP synthase III. Notably, xylerithiether outperformed norfloxacin against DNA gyrase B and fluconazole against sterol 14-α-demethylase. In vitro antibacterial activity was assessed for the purified compounds; all were active, predominantly against Gram-positive bacteria. These finding position *X. thienhirunae* SWUF17-44.1 as a promising source of bioactive metabolites and potential scaffolds for antimicrobial drug discovery.

Keywords: *Xylaria*; antimicrobial activity; LC-MS; molecular docking

Academic Editor: Alessio Cimmino

Received: 31 October 2025
Revised: 12 January 2026
Accepted: 14 January 2026
Published: 30 January 2026

1. Introduction

The genus *Xylaria* Hill ex Schrank (family Xylariaceae, order Xylariales) comprises a diverse group of saprophytic and endophytic fungi distributed primarily in tropical and subtropical regions. These fungi play crucial ecological roles in plant degradation and are prolific producers of structurally diverse secondary metabolites [1,2]. Over the past decade,

more than 400 compounds have been reported from *Xylaria* species, including alkaloids, cytochalasins, polyketides, terpenoids, xanthones, and phenolic derivatives [2]. Many of these metabolites exhibit notable biological activities, such as antimicrobial, antioxidant, cytotoxic, and anti-inflammatory effects, emphasizing the genus as a promising source of pharmaceutically relevant natural products [3–5]. However, most studies to date have focused on a limited number of identified species (*X. polymorpha, X. nigripes, X. curta, X. hypoxylon,* and *X. longipes*), which have yielded metabolites with diverse bioactivities, often derived from polyketide and phenolic pathways [2,3,5,6]. For example, extracts of *X. allantoidea* BCC23163 contained eremoxylarins D, F, and G with antimicrobial activity [7], *X. nigripes* produced xylapyrroside A with antibacterial activity [8], and curtachalasins X1 and X5 from *X. curta* E10 displayed cytotoxic effects [9]. Despite these advances, many *Xylaria* species remain chemically unexplored, and the structural novelty and mechanisms of action of their metabolites are still poorly understood, representing a significant knowledge gap in fungal natural product research.

The worldwide increase in antimicrobial resistance (AMR) further highlights the urgency of exploring under-investigated fungal taxa as potential sources of bioactive compounds, including new antimicrobial drugs. The World Health Organization has classified AMR as one of the top ten threats to global public health, causing an estimated 700,000 deaths annually, a number projected to rise to 40 million by 2050 without the development of new therapeutics [10]. Novel bioactive compounds and alternative drug targets are urgently needed. Several pathogenic bacterial enzymes have emerged as attractive candidates, including muramyl ligases (MurA-MurF), which catalyze steps in peptidoglycan biosynthesis and provide alternative targets to overcome β-lactam resistance [11]; dihydropteroate synthase (DHPS), a key enzyme in folate biosynthesis required for nucleotide production [12]; DNA gyrase and topoisomerase IV, which regulate DNA topology during replication and transcription [13,14]; and β-ketoacyl-acyl carrier protein synthase III (FabH), which initiates fatty acid biosynthesis and membrane lipid formation [15]. Inhibition of these essential and bacteria-specific enzymes can disrupt vital metabolic pathways and thereby weaken bacterial viability. Similarly, pathogenic fungi possess critical enzymes that serve as drug targets. Notable examples include sterol 14-α-demethylase, essential for ergosterol biosynthesis and membrane stability [16]; secreted aspartic proteinase-5, a virulence factor that facilitates host tissue invasion [17]; and UDP-N-acetylglucosamine pyrophosphorylase, which provides precursors for chitin biosynthesis and cell wall integrity [18]. Targeting these enzymes interferes with fungal survival and pathogenicity, offering promising avenues for antifungal drug development. Because pure metabolites are often available in only limited amounts, in silico molecular docking has become an increasingly valuable tool for prioritizing compounds for antimicrobial screening [19,20]. In addition to AMR, oxidative stress and chronic inflammation play central roles in infectious disease progression. Excessive production of reactive oxygen species can damage host tissues, while elevated nitric oxide levels intensify inflammation, compromise immune defences, and promote pathogen persistence. Natural products remain the most productive source of antimicrobial drugs, yet the discovery of novel scaffolds has slowed considerably, underscoring the importance of investigating neglected fungal taxa such as *Xylaria*.

In Thailand, several species, including *X. chaiyaphumensis*, *X. siamensis*, *X. subintraflava*, *X. thienhirunae*, and *X. vinacea*, have been reported from soil and termite nests, with extracts exhibiting strong antioxidant and anticancer activities [21,22]. Preliminary liquid chromatography–mass spectrometry analyses have indicated the presence of diverse bioactive metabolites; however, most remain unidentified and uncharacterized [22]. To address this gap, the present study focused on *X. thienhirunae* to comprehensively investigate its biological activities, including antimicrobial, antioxidant, and anti-inflammatory properties.

The crude extract was purified, and the isolated compounds were structurally identified and further evaluated using molecular docking against bacterial and fungal protein targets relevant to antimicrobial and antifungal activity.

2. Materials and Methods

2.1. Chemicals and Reagents

Ascorbic acid was obtained from ChemSupply (Gillman, Australia); Folin–Ciocalteu's reagent from Loba Chemie (Mumbai, India); and Griess reagent from Thermo Fisher Scientific (Waltham, MA, USA). The 2,2′-azino-bis(3-ethylbenzothiazoline-6-sulfonic acid) diammonium salt (ABTS), 2,2-diphenyl-1-picrylhydrazyl (DPPH), 6-hydroxy-2,5,7,8-tetramethylchroman-2-carboxylic acid (Trolox®), gallic acid, and resazurin sodium salt were purchased from Sigma-Aldrich (Burlington, MA, USA). Dimethyl sulfoxide (DMSO), ethanol, methanol (MeOH), and trifluoroacetic acid (TFA) were supplied by Fisher Scientific (Hampton, NH, USA). D-glucose anhydrous, malt extract, peptone, sodium carbonate (Na_2CO_3), and yeast extract were from Kemaus (Cherrybrook, Australia).

2.2. Xylaria thienhirunae SWUF17-44.1 Cultivation and Extraction

Pure culture of *X. thienhirunae* SWUF17-44.1, obtained from a previous study [21] and deposited in the Department of Microbiology, Faculty of Science, Srinakharinwirot University, Bangkok, Thailand, was used in this study. The isolate was initially cultivated on potato dextrose agar (PDA) at 30 °C for 3 weeks. Mycelial plugs were then transferred into yeast malt broth (30 L) and incubated at 30 °C for 6 weeks. After incubation, the mycelium was separated from the culture broth. The broth was extracted three times with ethyl acetate at a 1:1 (v/v) ratio. Ethyl acetate was selected because it has proven efficacy in recovering bioactive metabolites from *Xylaria* species [22]. The combined ethyl acetate extracts were concentrated under reduced pressure using a rotary evaporator at 50 °C. The resulting crude extract was subjected to biological activity assays.

2.3. Antibacterial Activity

The antibacterial activity of the ethyl acetate extract was assessed using a resazurin-based microdilution assay in 96-well plates, following Sarker et al. [23] with minor modifications. Standard bacterial strains (*Bacillus subtilis* ATCC 6633, *Escherichia coli* ATCC 35218, *Pseudomonas aeruginosa* ATCC 27853, and *Staphylococcus aureus* ATCC 25923) were adjusted to 5×10^6 CFU/mL. Extract concentrations ranged from 0.005 to 20 µg/µL. Each well contained 50 µL extract, 0.015% resazurin dye, Mueller–Hinton broth (MHB), and bacterial inoculum. Streptomycin was used as a positive control.

The minimum inhibitory concentration (MIC) was defined as the lowest concentration at which the resazurin dye remained blue, indicating growth inhibition. For minimum bactericidal concentration (MBC) determination, aliquots from wells at or near the MIC were spotted onto Mueller–Hinton agar (MHA) and incubated at 37 °C for 24 h. The MBC corresponded to the lowest concentration that completely inhibited visible growth. All assays were performed in triplicate.

2.4. Antifungal Activity

The antifungal activity of the ethyl acetate extract was evaluated using a resazurin-based microdilution assay in 96-well plates, following the protocols of Gharaghani et al. [24] and Staniszewska et al. [25], with modifications. MIC and minimum fungicidal concentration (MFC) values were determined against two *Candida* isolates (*C. albicans* TISTR 5554 and *C. tropicalis* TISTR 5136) obtained from the Thailand Institute of Scientific and Technological Research (TISTR). Both strains were cultured in yeast extract peptone dextrose (YEPD)

broth and incubated at 30 °C. After 20 h of incubation, cells were harvested by centrifugation at 3000 rpm for 5 min at 4 °C, washed with sterile distilled water, and adjusted to a final concentration of 4.0×10^8 CFU/mL. Extract concentrations ranged from 0.049 to 100 μg/μL. Each well contained the same mixture as described in Section 2.3. Fluconazole (0.8 mg/mL) was used as the positive control. The MFC was determined by streaking aliquots from wells at or near the MIC onto YEPD agar plates and incubating at 30 °C for 24 h; the MFC was defined as the lowest concentration showing no visible *Candida* growth. All assays were performed in triplicate.

2.5. Antioxidant Activities

2.5.1. 2,2-Diphenyl-1-picrylhydrazyl (DPPH) Radical Scavenging Assay

The antioxidant activity of the extract was evaluated using the DPPH radical assay, as described by Wangsawat et al. [22], with some modifications. Fifty microliters of extract in methanol (MeOH) were subjected to two-fold serial dilutions in 96-well plates, after which 150 μL of 2 mM DPPH solution was added to each well. The mixtures were incubated in the dark at room temperature for 30 min, and absorbance was measured at 517 nm using a microplate reader. Trolox and MeOH were used as the positive and blank controls, respectively. All assays were performed in triplicate. The percentage of radical scavenging activity was calculated as:

$$\text{Inhibition (\%)} = [(\text{Ac} - \text{As})/\text{Ac}] \times 100$$

where Ac is the absorbance of the control and As is the absorbance of the sample. The IC_{50} value was defined as the concentration required to inhibit 50% of DPPH radicals.

2.5.2. 2,2′-Azino-bis(3-ethylbenzothiazoline-6-sulfonic Acid) Diammonium Salt (ABTS) Radical Scavenging Assay

Antioxidant activity was also determined using the ABTS assay, as described by Wangsawat et al. [22] with modifications. Twenty-five microliters of extract in distilled water were serially diluted two-fold in 96-well plates. An $ABTS^{\bullet+}$ solution was then added to each well to a final volume of 176 μL, adjusted to an absorbance of 0.7 at 734 nm. Plates were incubated in the dark for 7 min, after which absorbance was recorded at 734 nm. Trolox was used as the positive control. All assays were conducted in triplicate, and the percentage inhibition was calculated using the same formula as for the DPPH assay.

2.6. Total Phenolic Content (TPC)

TPC of the ethyl acetate extract was measured using the Folin–Ciocâlteu method, as described by Rusu et al. [26] with modifications. Each well contained 20 μL of extract, 100 μL of 10% (*v*/*v*) Folin–Ciocâlteu reagent, and 80 μL of 7.5% (*w*/*v*) sodium carbonate. The mixtures were incubated at room temperature for 30 min, and absorbance was measured at 735 nm. Gallic acid was used as the standard, and results were expressed as μg gallic acid equivalents per mg of extract (μg GAE/mg extract). All assays were performed in six replicates.

2.7. Anti-Inflammatory Activity

The anti-inflammatory activity was determined using a nitric oxide (NO) radical scavenging assay, following a modified protocol of Karin et al. [27]. Briefly, the extract was mixed with 60 μL of 10 mM sodium nitroprusside ($Na_2[Fe(CN)_5NO]\cdot H_2O$) and incubated at room temperature for 150 min. Then, 100 μL of Griess reagent was added, and the mixture was incubated for an additional 30 min at room temperature. Absorbance was measured at 540 nm using a microplate reader. All reactions were carried out in triplicate. The percentage of NO inhibition was calculated using the same formula described in Section 2.5.

2.8. Statistical Analysis

All data were expressed as mean ± standard deviation (SD). Statistical differences between treatments were analyzed using Student's *t*-test in SPSS software version 25. A p-value < 0.05 was considered statistically significant.

2.9. Liquid Chromatography–Mass Spectrometry (LC-MS) Analysis

The chemical profile of the extract was analyzed by high-resolution LC-MS, following Wangsawat et al. [22] with modifications. The extract was dissolved in LC-MS grade methanol at 0.01 mg/mL, filtered through a 0.22 µm syringe filter, and subjected to analysis using an Agilent reversed-phase LC system equipped with a Phenomenex C18(2) 100 Å column (Agilent, Santa Clara, CA, USA) (150 × 4.6 mm). Chromatographic conditions were as follows: column temperature, 25 °C; flow rate, 0.7 mL/min; injection volume, 20 µL; and UV-Vis detection at 220–310 nm. The mobile phase consisted of 0.1% formic acid in water (solvent A) and acetonitrile (solvent B), with a gradient elution from 10% to 90% solvent B over 30 min.

High-resolution mass spectrometry was performed using a quadrupole time-of-flight (Q-TOF) mass spectrometer with an electrospray ionization (ESI) source, operated in positive ion mode. The parameters were as follows: gas temperature, 300 °C; drying gas flow, 8 L/min; nebulizer pressure, 35 psi; and fragmentor voltage, 175 V. The mass range was set from 100 to 1500 m/z. Data acquisition and processing were carried out using Agilent MassHunter Qualitative Analysis 10.0 software, and metabolite peaks were tentatively identified by comparison with the METLIN database.

2.10. Isolation, Purification, and Structure Elucidation of Compounds

The ethyl acetate extract was fractionated by solid-phase extraction (SPE) using 100% MeOH. The collected fraction was dissolved in MeOH (50 mg/mL), filtered through a 0.22 µm syringe filter, and subjected to preparative HPLC on a Phenomenex C18 column (150 × 21.2 mm, 10 mm). The mobile phase consisted of MeOH and water containing 0.1% trifluoroacetic acid (TFA), with a gradient from 30% MeOH to 100% MeOH over 40 min. Chromatographic conditions were as follows: injection volume, 100–400 µL; column temperature, 25 °C; flow rate, 10 mL/min; and UV-Vis detection at 220–310 nm. Collected peaks were checked for purity by analytical HPLC before structural elucidation.

Pure compounds were characterized by one-dimensional (^{1}H and ^{13}C NMR) and two-dimensional NMR spectroscopy, including ^{1}H–^{1}H correlation spectroscopy (COSY), heteronuclear single quantum coherence (HSQC), and heteronuclear multiple bond correlation (HMBC). Molecular masses were confirmed by mass spectrometry (Waters Micromass LCT) with MassLynx version 4.1 software, operated in both positive and negative ion modes.

2.11. Molecular Docking

The 3D structures of isolated compounds (ligands) were docked against selected bacterial and fungal protein targets obtained from the RCSB Protein Data Bank (PDB) (https://www.rcsb.org/). Bacterial targets included muramyl ligase E (MurE; PDB IDs: 4C12, 7B9E), dual muramyl ligases D and E (MurD/MurE; PDB ID: 2Y1O), dihydropteroate synthase (DHPS; PDB IDs: 1AD4, 5V7A), DNA gyrase B (PDB IDs: 4URN, 6F86), topoisomerase IV (PDB ID: 4HZ0), and β-ketoacyl-acyl carrier protein synthase III (FabH; PDB ID: 2QO0). Fungal targets included sterol 14-α-demethylase (CYP51; PDB ID: 5TZ1), secreted aspartic proteinase-5 (SAP5; PDB ID: 2QZX), and UDP-N-acetylglucosamine pyrophosphorylase (UAP1; PDB ID: 6G9V) (Table S1).

Docking simulations were performed using GOLD 5.3.0. Receptor validation was confirmed when the GoldScore fitness function was high and the root mean square devi-

ation (RMSD) of re-docked ligands was <2 Å, indicating reliable docking accuracy. The best docking poses, based on the highest GoldScore values for each compound–protein interaction, were visualized and analyzed using BIOVIA Discovery Studio Visualizer [28].

3. Results

3.1. Antimicrobial Activity of X. thienhirunae SWUF17-44.1 Extract

The ethyl acetate extract of *X. thienhirunae* SWUF17-44.1 culture broth yielded 0.318 g/L and exhibited antimicrobial activity against four bacterial strains (*B. subtilis* ATCC6633, *S. aureus* ATCC25923, *E. coli* ATCC35218, and *P. aeruginosa* ATCC27853) and two fungal pathogens (*C. albicans* TISTR5554 and *C. tropicalis* TISTR5136) (Table 1). The extract was most effective against the Gram-positive bacteria, *S. aureus* (MIC = 0.63 μg/μL) and *B. subtilis* (MIC = 1.25 μg/μL), whereas the Gram-negative bacteria, *E. coli* and *P. aeruginosa*, showed MIC values of 2.5 and 5 μg/μL, respectively. Antifungal activity was observed against *C. albicans* and *C. tropicalis* with MIC values of 6.25 μg/μL.

Table 1. Antimicrobial activity of the ethyl acetate extract of *X. thienhirunae* SWUF17-44.1 expressed as minimum inhibitory concentration (MIC) and minimum bactericidal concentration (MBC) or minimum fungicidal concentration (MFC).

Bacterial and Fungal Strains	MIC (MBC or MFC) Values in μg/μL
B. subtilis ATCC6633	1.25 (2.5)
E. coli ATCC35218	2.5 (5)
P. aeruginosa ATCC27853	5 (10)
S. aureus ATCC25923	0.63 (5)
C. albicans TISTR5554	6.25 (12.5)
C. tropicalis TISTR5136	6.25 (12.5)

3.2. Antioxidant Activity, Anti-Inflammatory Effect, and Total Phenolic Content

The antioxidant activity of the ethyl acetate extract was assessed using both DPPH and ABTS assays. The extract exhibited IC_{50} values of 0.706 ± 0.022 μg/μL and 0.251 ± 0.019 μg/μL, respectively, compared with the positive control Trolox, which showed IC_{50} values of 0.002 μg/μL (DPPH) and 0.013 μg/μL (ABTS) (Figure 1). Although less potent than Trolox, the extract demonstrated notable free radical scavenging activity. The TPC of the extract, expressed as gallic acid equivalents (GAE) (Figure S1), was 56.486 ± 5.642 μg GAE/mg extract. In addition, the extract exhibited anti-inflammatory activity, with NO inhibition of 16.737 ± 2.479% at a concentration of 12.8 μg/mL.

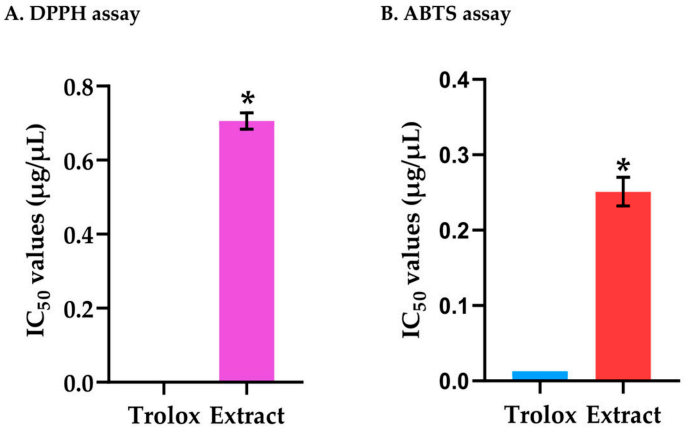

Figure 1. Antioxidant activity of the ethyl acetate extract of *X. thienhirunae* SWUF17-44.1: (**A**) DPPH assay, and (**B**) ABTS assay. Data are presented as mean ± standard deviation. * indicates significant differences ($p < 0.05$).

3.3. Liquid Chromatography–Mass Spectrometry (LC-MS)

LC-MS analysis of the ethyl acetate extract yielded a total ion chromatogram with 13 distinct peaks in positive ion mode (Figure 2) and 4 peaks in negative ion mode (Figure S2). Comparison of the mass spectra with database entries enabled the tentative identification of eight compounds in positive mode: *p*-acetamidophenol, aminoparathion, istamycin C1, kolanone, 2-(4-methyl-5-thiazolyl)ethylbutanoate, netilmicin, octylamine, and westiellamide (Table 2). The remaining five peaks (peaks 1, 2, 9, 10, and 11) showed masses corresponding to more than one candidate compound and therefore could not be assigned unambiguously. For example, peak 1 (m/z 268.1035) matched several possible metabolites, including zidovudine, adenosine, 2′-deoxyguanosine, and vidarabine, while peak 2 (m/z 192.1368) corresponded to either lupinine or nitramine. These peaks were thus classified as unidentified. In negative ion mode, only two compounds, 5-aminoimidazole and 2-thiophenecarboxaldehyde, were tentatively annotated (Table S2).

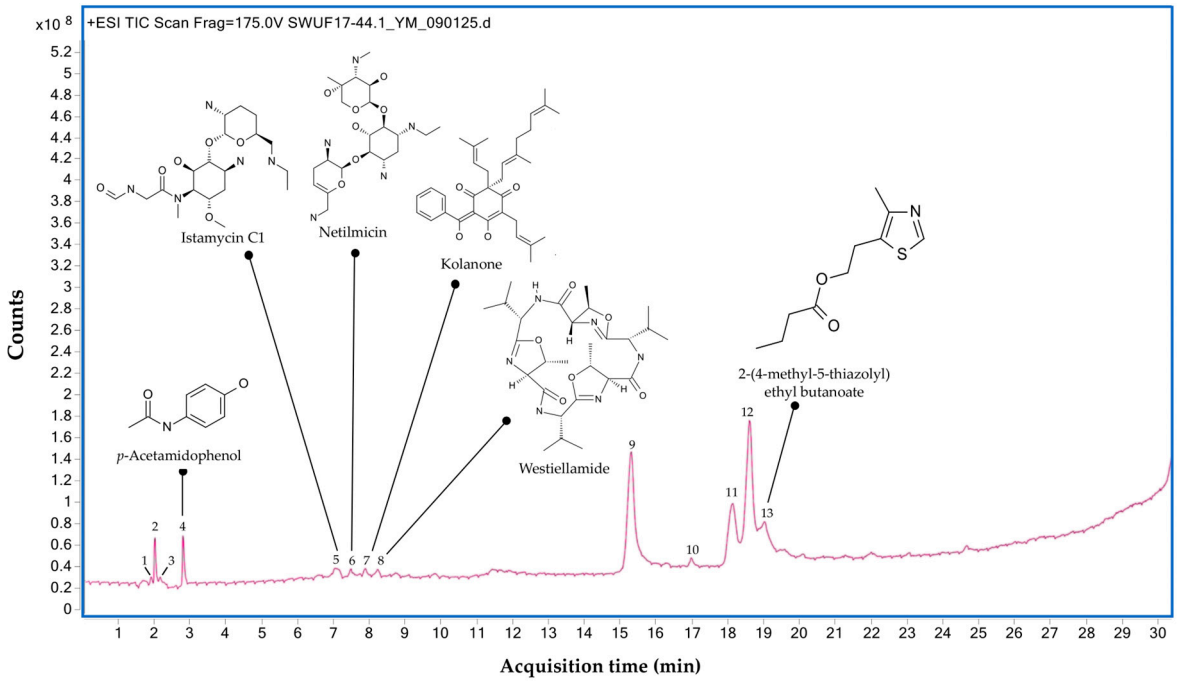

Figure 2. Total ion chromatogram (TIC) of the ethyl acetate extract of *X. thienhirunae* SWUF17-44.1 showing peaks 1–13 corresponding to putatively annotated metabolites identified by LC-MS analysis.

Table 2. Mass spectra data of separated and predicted peaks from *X. thienhirunae* SWUF17-44.1 in positive ion mode.

Peak No.	Retention Time (min)	Mass (m/z)	Identified Compounds	Molecular Formula	Biological Properties	References
1	1.87–1.96	268.1035	Zidovudine, adenosine, 2′-deoxyguanosinevidarabine, vidarabine	-	-	-
2	1.97–2.09	192.1368	Lupinine, nitramine	-	-	-
3	2.12–2.22	130.1585	Octylamine	$C_8H_{19}N$	-	-
4	2.75–2.90	174.0534	*p*-Acetamidophenol	$C_8H_9NO_2$	anti-inflammatory activity, antibacterial and antifungal activities	Hinz et al. [29], Ahmad et al. [30]
5	6.93–7.24	432.2795	Istamycin C1	$C_{19}H_{37}N_5O_6$	antibiotic	Ikeda et al. [31]
6	7.41–7.59	476.3064	Netilmicin	$C_{21}H_{41}N_5O_7$	aminoglycoside antibiotic	Miller et al. [32]
7	7.81–7.97	503.3059, 520.3326	Kolanone	$C_{33}H_{42}O_4$	antimicrobial drug	Hussain et al. [33]

Table 2. *Cont.*

Peak No.	Retention Time (min)	Mass (*m*/*z*)	Identified Compounds	Molecular Formula	Biological Properties	References
8	8.19–8.34	564.3588, 547.3323	Westiellamide	$C_{27}H_{42}N_6O_6$	antimicrobial activity, cytotoxicity	Prinsep et al. [34]
9	15.14–15.65	311.2693	5b-Pregnanediol, pentadecylbenzene	-	-	-
10	16.93–17.14	230.2476	2-Tetradecanone, 12-methyltridecanal	-	-	-
11	17.97–18.32	198.1847	(3Z,6Z,9Z)-Dodecatrienol, homodihydrojasmone, 2-trans-6-cis-dodecadienal, cis-quinceoxepane, tricycloekasantalol, (2E,4E)-2,4-dodecadienal	-	-	-
12	18.45–18.85	279.0931	Aminoparathion	$C_{10}H_{16}NO_3PS$	-	-
13	18.92–19.18	214.0891	2-(4-Methyl-5-thiazolyl)ethyl butanoate	$C_{10}H_{15}NO_2S$	antimicrobial activities	Singh et al. [35]

3.4. Isolation, Purification, and Structure Elucidation of Compounds from X. thienhirunae SWUF17-44.1

The ethyl acetate extract of *X. thienhirunae* SWUF17-44.1 was subjected to chromatographic isolation and purification, yielding four pure compounds: two previously known and two novel metabolites (Figure S3), described as follows.

Compound **1** was obtained as a brown, viscous gum. Its molecular formula, $C_{12}H_{18}O_4$ (226.2689), was established from the pseudomolecular ion $[M + Na]^+$ at *m*/*z* 249.1103 in positive ESI-MS. Structure elucidation was performed using 1D (^{1}H, DEPTQ) and 2D (COSY, HSQC, HMBC) NMR spectroscopy (Figures 3A and S4, Table S3). The ^{1}H NMR spectrum displayed signals for two methyl groups (δ_H 1.78 s, 1.75 s), two oxymethylenes (δ_H 4.51 s, 4.22 dd, 3.91 dd), one oxymethine (δ_H 3.72 dd), and an aromatic region consistent with a *para*-disubstituted benzene ring (δ_H 7.26 d, J = 8.6 Hz; 6.92 d, J = 8.6 Hz). The DEPTQ spectrum confirmed 12 carbons, including two methyls (δ_C 25.3, 23.6), two oxymethylenes (δ_C 63.5, 69.1), one oxymethine (δ_C 76.3), one oxygenated quaternary carbon (δ_C 74.0), two aromatic quaternary carbons (δ_C 133.5, 158.8; one oxygenated), and four aromatic methines (δ_C 114.2 ×2, 128.3 ×2). HMBC correlations such as H-2 ⟶ C-3 (^2J), C-6 & 7 (^3J), and C-5 (^4J), H-7 ⟶ C-1 (^2J), and C-2 (^3J), and H-1′ ⟶ C-4 and C-2′ (^2J) supported the proposed skeleton. No matches were found in CHEMnetBASE or SciFinder, confirming this metabolite as a novel natural product, herein named xylerithienol.

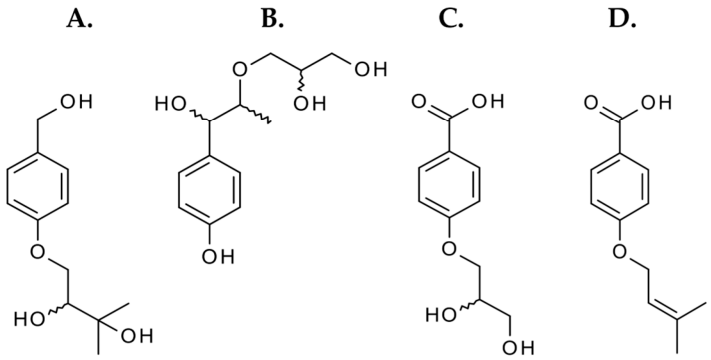

Figure 3. Chemical structures from ethyl acetate extract of *X. thienhirunae* SWUF17-44.1 (**A**) xylerithienol, (**B**) xylerithiether, (**C**) 4-(2,3-dihydroxypropoxy)benzoic acid, and (**D**) 4-prenyloxybenzoic acid.

Compound **2** was also isolated as a brown, viscous gum. Its molecular formula, $C_{12}H_{18}O_5$ (MW 242.2683), was deduced from the pseudomolecular ion $[M + H]^+$ at *m*/*z* 243.0943 in positive ESI-MS. Structure elucidation by 1D and 2D NMR (Figures 3B and S5,

Table S3) revealed ^{1}H signals for a methyl group (δ_H 1.11 d), two oxymethines (δ_H 4.42 d, 5.37 m), two oxymethylenes (δ_H 4.42 d, 3.83 m), and aromatic protons consistent with a *para*-disubstituted benzene ring (δ_H 7.27 m, J = 8.5 Hz; 6.89 m, J = 8.8 Hz). The DEPTQ spectrum showed 12 carbons, including a methyl (δ_C 17.8), two oxymethylenes (δ_C 65.5, 75.0), three oxymethines (δ_C 71.0, 77.3, 86.6), two quaternary carbons (δ_C 134.3, 157.7; one oxygenated), and four aromatic methines (δ_C 114.3 ×2, 127.9 ×2). HMBCs such as H-2 ⟶ C-3 & H-6 ⟶ C-5 (^2J), H-2 ⟶ C-4 (^3J), H-3 ⟶ C-4 (^2J) and C-6 (^4J), H-1′ ⟶ C-6 and C-2′ (^{2}J), and C-5 (^3J), H-3′ ⟶ C-2′ (^2J), H-1″ ⟶ C-2″ (^2J), H-1″ ⟶ C-2′ and C-3″ (^3J), and H-1″ ⟶ C-1′ (^4J), and H-2″⟶ C-3″ (^2J) further supported the structure. No database matches were found, and the compound was designated as a new metabolite, xylerithiether.

Compound **3** was isolated as a brown amorphous powder. The pseudomolecular ion $[M + H]^+$ at m/z 213.0416 corresponded to $C_{10}H_{12}O_5$. NMR analysis (Figures 3C and S6, Table S3) revealed two oxymethylenes (δ_H 4.80 m, 4.62 m), one oxymethine (δ_H 5.40 m), and aromatic signals of a *para*-disubstituted benzene ring (δ_H 7.95 d, J = 8.9 Hz; 6.97 d, J = 8.9 Hz). DEPTQ spectra confirmed 10 carbons, including one methylene (δ_C 75.3), one methine (δ_C 86.2), one oxymethylene (δ_C 65.5), four aromatic methines (δ_C 114.1 ×2, 131.3 ×2), and two aromatic quaternary carbons (δ_C 162.2; one oxygenated). HMBC analysis indicated the presence of a carboxylic acid carbon, establishing the structure as 4-(2,3-dihydroxypropoxy)benzoic acid.

Compound **4** was obtained as a light-yellow amorphous powder. ESI-MS in both positive and negative modes showed ions at m/z 207.0962 $[M + H]^+$, 229.0636 $[M + Na]^+$, and 205.0783 $[M - H]^-$, consistent with $C_{12}H_{14}O_3$. The ^{1}H NMR spectrum displayed signals for two methyl groups (δ_H 1.78 s, 1.75 s), one methylene (δ_H 4.59 d, J = 6.7 Hz), one methine (δ_H 5.46 t, J = 5.5 Hz), and a para-disubstituted benzene ring (δ_H 7.94 d, J = 8.9 Hz; 6.95 d, J = 8.9 Hz). DEPTQ confirmed 12 carbons, including two methyls (δ_C 24.4, 16.8), one oxymethylene (δ_C 64.6), one methine (δ_C 119.2), two quaternary carbons (δ_C 122.6, 137.9), four aromatic methines (δ_C 114.0 ×2, 131.4 ×2), and one carboxylic acid carbon (δ_C 168.7). Based on COSY, HSQC, and HMBC correlations, the compound was identified as the known metabolite 4-prenyloxybenzoic acid (Figures 3D and S7, Table S3).

3.5. Molecular Docking of Four Compounds Against Target Proteins

The extracts of *X. thienhirunae* SWUF17-44.1 exhibited antimicrobial activity against both bacterial strains and fungal pathogens. To further elucidate the underlying mechanisms, molecular docking was performed, which revealed strong binding affinities of four isolated compounds toward several key bacterial and fungal protein targets (Tables 3 and 4). Xylerithiether exhibited the strongest overall binding among the tested compounds. Against Gram-positive bacteria, it achieved the highest docking score with MurE (PDB ID: 4C12; score 96.15), surpassing the reference antibiotics ampicillin, amoxicillin, and carbenicillin (Figures 4 and S8). It also showed notable activity against the dual MurD/MurE target (PDB ID: 2Y1O; score 65.60), higher than reference antibiotics. For topoisomerase-related targets, xylerithiether produced a superior docking score against topoisomerase IV (PDB ID: 4HZ0; score 63.60), outperforming norfloxacin. Comparable results were obtained against DNA gyrase B (PDB ID: 6F86), where its binding exceeded that of norfloxacin. Additionally, xylerithiether demonstrated the highest affinity for β-ketoacyl-ACP synthase III (FabH; PDB ID: 2QO0; score 68.40), surpassing the standard ligand and isoniazid. In fungal docking studies, xylerithiether again ranked highest, showing strong interactions with sterol 14-α-demethylase (PDB ID: 5TZ1; score 83.23), exceeding fluconazole (Figure 5A–C). It also exhibited superior binding to secreted aspartic proteinase-5 (PDB ID: 2QZX) and UDP-N-acetylglucosamine pyrophosphorylase (PDB ID: 6G9V), suggesting potential to disrupt fungal virulence and cell wall biosynthesis.

Table 3. Molecular docking GoldScores of four compounds isolated from *X. thienhirunae* SWUF17-44.1 against selected antibacterial target proteins.

Targeted Protein	PDB Code	Ligand's Protein	Compounds				Antibiotics					
			Xylerithienol	Xylerithiether	4-(2,3-Dihydroxypropoxy)benzoic Acid	4-Prenyloxybenzoic Acid	Ampicillin	Amoxicillin	Carbenicillin	Norfloxacin	Sulfonamide	Isoniazid
muramyl ligase E (G+)	4C12	131.85 [a]	89.58	96.15	89.56	57.40	65.15	61.79	60.21	-	-	-
muramyl ligase E (G−)	7B9E	49.12 [b]	46.17	48.51	41.11	41.61	60.32	59.80	58.32	-	-	-
Dual MurD & MurE	2Y1O	87.04 [c]	63.15	65.60	64.07	42.02	49.05	53.61	53.64	-	-	-
dihydropteroate synthase (G+)	1AD4	84.52 [d]	72.66	78.77	68.09	52.17	-	-	-	-	42.48	-
dihydropteroate synthase (G−)	5V7A	59.03 [e]	57.34	62.85	56.91	42.76	-	-	-	-	45.57	-
gyrase B (G+)	4URN	91.22 [f]	59.71	66.27	57.60	48.79	-	-	-	61.04	-	-
gyrase B (G−)	6F86	77.18 [g]	44.76	57.50	44.86	39.89	-	-	-	48.82	-	-
topoisomerase IV	4HZ0	60.98 [h]	58.91	63.60	67.94	51.70	-	-	-	52.55	-	-
β-ketoacyl-acyl carrier protein synthase III	2QO0	70.37 [i]	56.23	68.40	60.94	50.93	-	-	-	-	-	38.45

[a] Adenosine-5′-diphosphate, [b] 4-chloro-N-cyclopentyl-1-methyl-1H-pyrazole-3-carboxamide, [c] (2r)-2-[[3-[[4-[(z)-(4-oxo-2-sulfanylidene-1,3-thiazolidin-5-ylidene)methyl]phenyl]methylamino]phenyl]carbonylamino]pentanedioic acid, [d] 6-hydroxymethylpterin-diphosphate, [e] [(2-amino-9-methyl-6-oxo-6,9-dihydro-1H-purin-8-yl)sulfanyl]acetic acid, [f] Novobiocin, [g] 4-(4-bromanylpyrazol-1-yl)-6-(ethylcarbamoylamino)-~{*N*}-pyridin-3-yl-pyridine-3-carboxamide, [h] 7-(1H-imidazol-1-yl)-2-(pyridin-3-yl)[1,3]thiazolo[5,4-d]pyrimidin-5-amine, and [i] Decane-1-thiol.

Table 4. Molecular docking GoldScores of the four compounds isolated from *X. thienhirunae* SWUF17-44.1 against selected antifungal target proteins.

Targeted Protein	PDB Code	Ligand's Protein	Compounds				Antibiotics
			Xylerithienol	Xylerithiether	4-(2,3-Dihydroxypropoxy) benzoic Acid	4-Prenyloxybenzoic Acid	Fluconazole
sterol 14-alpha demethylase	5TZ1	152.23 [a]	73.68	83.23	75.23	55.28	58.24
secreted aspartic proteinase-5	2QZX	82.56 [b]	61.76	64.70	57.69	41.58	46.09
UDP-N-acetylglucosamine pyrophosphorylase	6G9V	111.56 [c]	54.33	69.25	58.19	48.47	47.07

[a] Protoporphyrin IX Containing Fe; [b] Pepstatin; [c] Uridine-Diphosphate-N-Acetylglucosamine pyrophosphorylase.

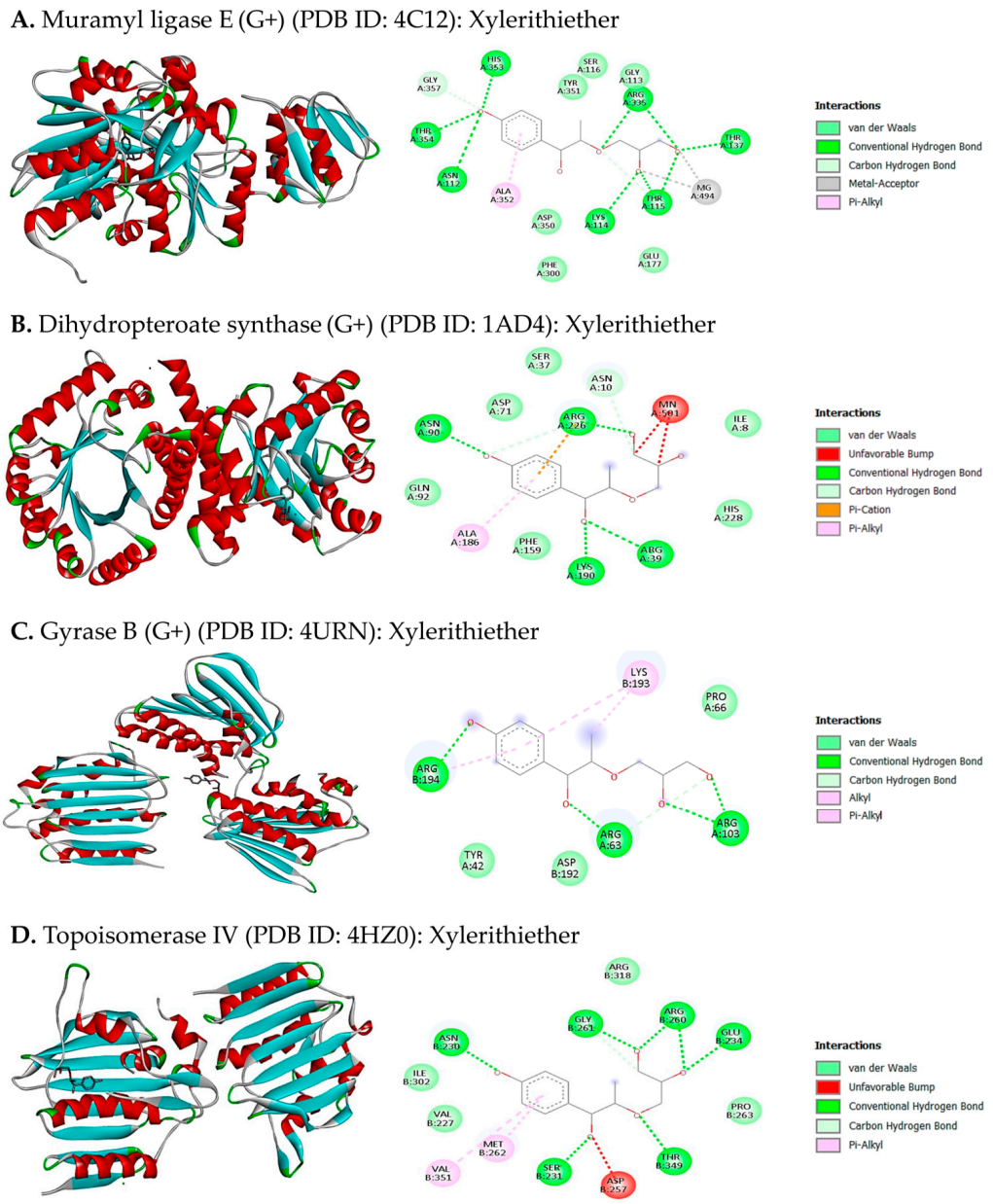

Figure 4. Molecular docking visualization of xylerithiether with representative antibacterial target proteins based on GoldScore results. (**A**) muramyl ligase E (G+), (**B**) dihydropteroate synthase (G+), (**C**) gyrase B (G+), and (**D**) topoisomerase IV.

Xylerithienol also showed consistently strong binding. Against Gram-positive MurE (4C12), it outperformed reference antibiotics, while docking to dual MurD/MurE (2Y1O; score 63.15) yielded comparable results to xylerithiether (Figures 6 and S9). For topoisomerase targets, xylerithienol achieved the score against DNA gyrase B (PDB ID: 4URN; score: 59.71) and exceeded norfloxacin against DNA gyrase B (6F86). It also demonstrated favourable interaction with FabH (2QO0). In fungal targets, xylerithienol scored above fluconazole against sterol 14-α-demethylase (5TZ1) and exhibited superior binding to secreted aspartic proteinase-5 (2QZX). It also bound UDP-N-acetylglucosamine pyrophosphorylase (6G9V), supporting its role in interfering with fungal cell wall formation (Figure 5D–F).

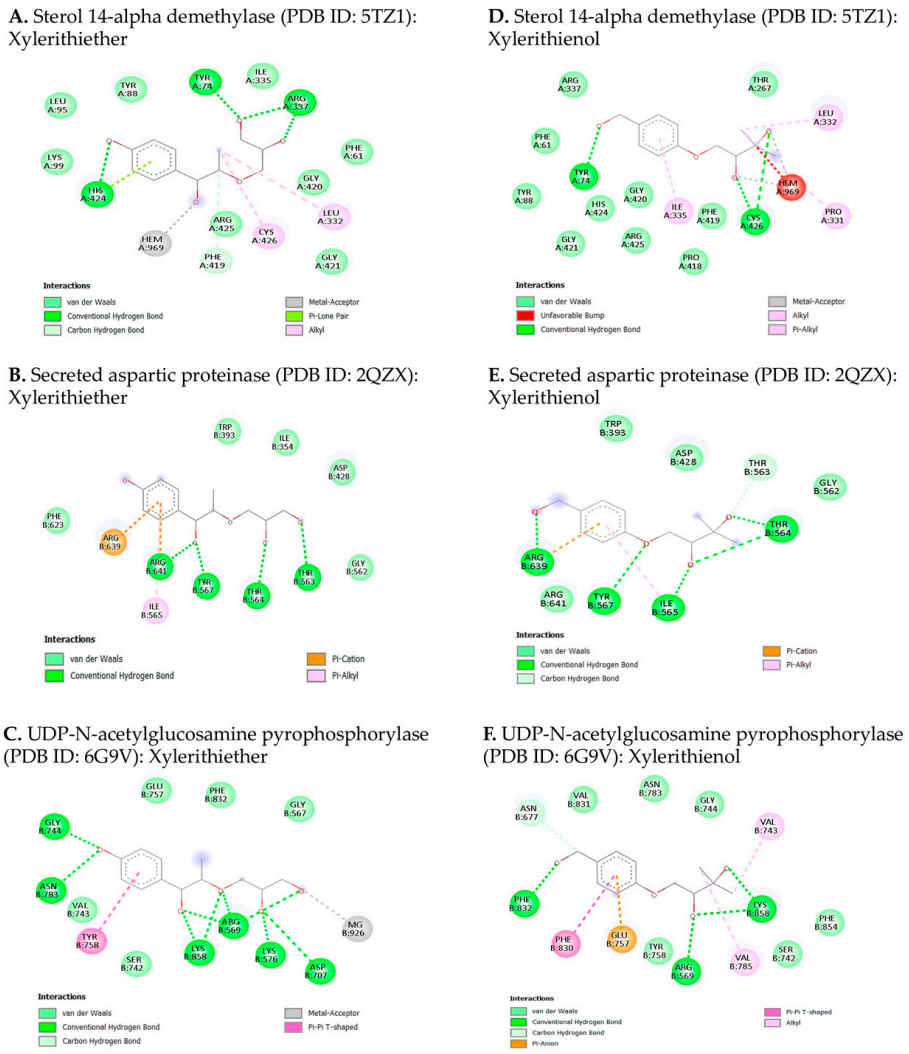

Figure 5. Molecular docking visualization of xylerithiether and xylerithienol with representative antifungal target proteins based on GoldScore results. (**A**,**D**) sterol 14-alpha demethylase, (**B**,**E**) secreted aspartic proteinase-5, and (**C**,**F**) UDP-N-acetylglucosamine pyrophosphorylase.

For 4-(2,3-dihydroxypropoxy)benzoic acid, it displayed moderate to strong binding. Against Gram-positive MurE (4C12), it scored higher than reference antibiotics, and against MurD/MurE (2Y1O; score 64.07), its score exceeded amoxicillin. It also produced favourable results for DNA gyrase B (4URN) and FabH (2QO0; 57.60–60.94). In fungi, 4-(2,3-dihydroxypropoxy)benzoic acid exhibited docking scores higher than fluconazole for sterol 14-α-demethylase (5TZ1), and showed strong binding to secreted aspartic proteinase-5 (2QZX) and UDP-N-acetylglucosamine pyrophosphorylase (6G9V) (Figures S10 and S11).

The 4-prenyloxybenzoic acid demonstrated the weakest interactions among the isolates. Against Gram-positive MurE (4C12), its docking score was lower than the reference antibiotics. Similarly, against MurE of Gram-negative bacteria (7B9E), its scores were inferior to those of the antibiotics. For dihydropteroate synthase (5V7A), its score (42.76) was below the reference sulfonamide (45.57). It also yielded lower values for topoisomerase and FabH compared with other test compounds. Nevertheless, 4-prenyloxybenzoic acid showed moderate binding to fungal sterol 14-α-demethylase (5TZ1) and secreted aspartic proteinase-5 (2QZX), although its scores were lower than those of xylerithiether, xylerithienol, and 4-(2,3-dihydroxypropoxy)benzoic acid (Figures S12 and S13).

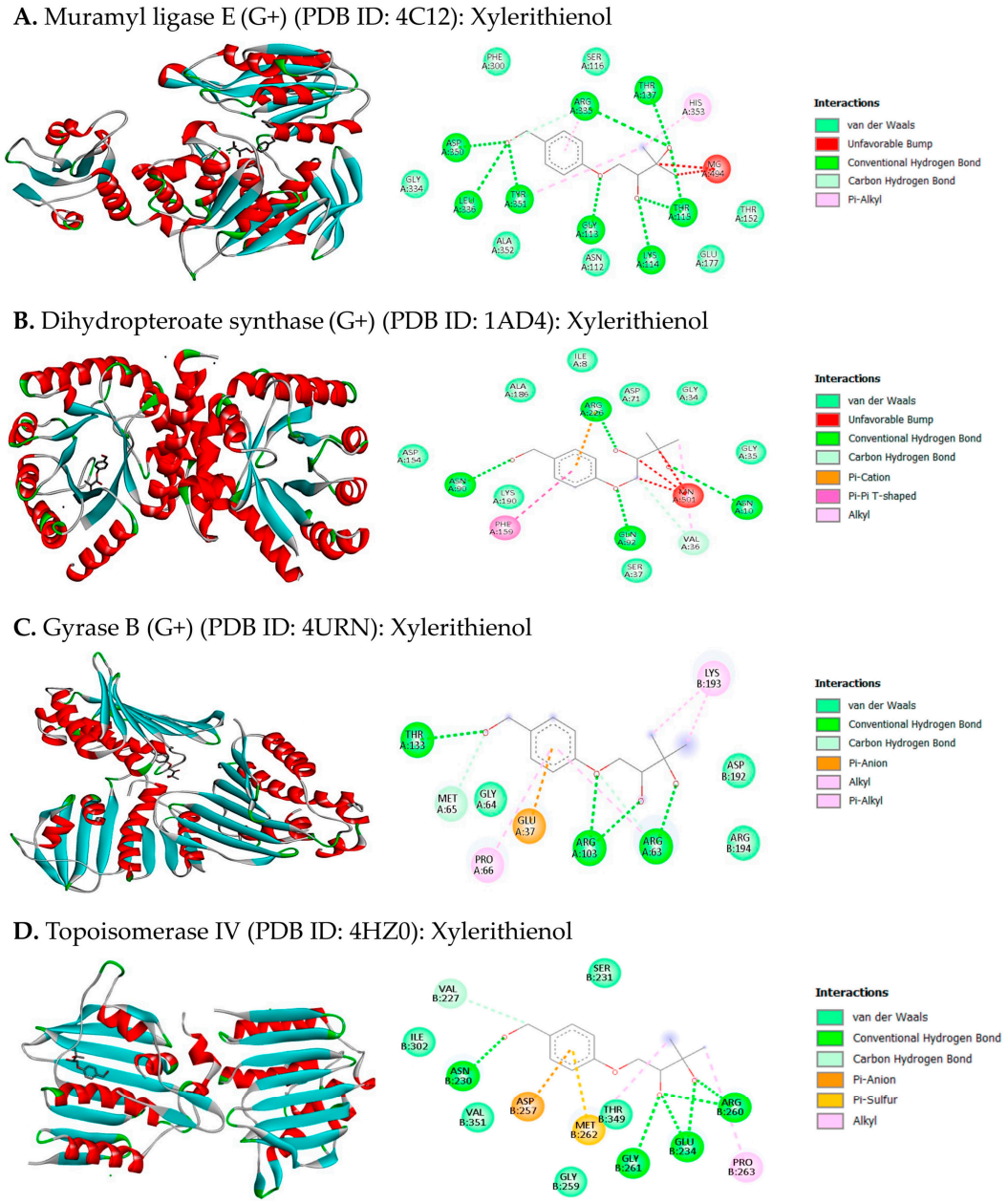

Figure 6. Molecular docking visualization of xylerithienol with representative antibacterial target proteins based on GoldScore results. (**A**) muramyl ligase E (G+), (**B**) dihydropteroate synthase (G+), (**C**) gyrase B (G+), and (**D**) topoisomerase IV.

3.6. Antimicrobial Activity of the Purified Compounds

Four purified compounds were evaluated for antimicrobial activity to support the in silico docking predictions, with ampicillin used as the positive control. All compounds inhibited Gram-positive bacteria, with MICs ranging from 0.625 to 10 µg/µL, whereas Gram-negative strains generally exhibited higher MIC values (Tables 5 and S4). 4-(2,3-Dihydroxypropoxy)benzoic acid showed the lowest MIC against *B. subtilis* (0.625 µg/µL) and an MIC of 1.25 µg/µL against *S. aureus*, whereas xylerithiether showed the lowest MIC against *S. aureus* (0.625 µg/µL) and an MIC of 1.25 µg/µL against *B. subtilis*. Xylerithienol displayed MICs of 1.25 µg/µL and 5 µg/µL against *S. aureus* and *B. subtilis*, respectively, while 4-prenyloxybenzoic acid was less active (MICs of 5 and 10 µg/µL, respectively). In contrast, ampicillin showed substantially higher potency, with MICs ranging from 0.016 to 0.5 µg/µL. Overall, the observed activity trend was consistent with the docking results, which predicted stronger binding to Gram-positive targets (e.g., MurE and dihydropteroate

synthase) than to the corresponding Gram-negative enzymes. Due to limited compound availability, antifungal assays against *C. albicans* and *C. tropicalis* could not be performed.

Table 5. Antibacterial activity of the purified compounds of *X. thienhirunae* SWUF17-44.1 expressed as minimum inhibitory concentration (MIC) and minimum bactericidal concentration (MBC).

Bacterial Strains	MIC (MBC) Values in μg/μL				
	Xylerithiether	Xylerithienol	4-(2,3-Dihydroxypropoxy)benzoic Acid	4-Prenyloxybenzoic Acid	Ampicillin
B. subtilis ATCC6633	1.25 (1.25)	5 (5)	0.625 (0.625)	10 (10)	0.016 (0.016)
S. aureus ATCC25923	0.625 (>5)	1.25 (>10)	1.25 (5)	5 (>10)	0.031 (0.250)
E. coli ATCC35218	>2.5 (>2.5)	10 (>10)	>2.5 (>2.5)	>10 (>10)	2 (2)
P. aeruginosa ATCC27853	>2.5 (>2.5)	10 (>10)	>2.5 (>2.5)	>10 (>10)	0.5 (2)

4. Discussion

This study presented the first comprehensive investigation of the biological activities and chemical composition of *X. thienhirunae* SWUF17-44.1 extract. The extract demonstrated broad-spectrum antimicrobial activity, with greater efficacy against Gram-positive bacteria than Gram-negative strains. The lowest MIC values were observed for *S. aureus* (0.63 μg/μL) and *B. subtilis* (1.25 μg/μL), consistent with the general susceptibility of Gram-positive bacteria to natural products due to the absence of an outer membrane barrier. In contrast, *E. coli* and *P. aeruginosa* required higher MIC values (2.5–5 μg/μL), which may be attributed to the structural complexity of the Gram-negative cell wall. Comparable antimicrobial activities have been reported from other *Xylaria* species. For example, the endophytic *Xylaria* sp. FPL-25, isolated from *Ficus pumila* Linn., produced xylobovide-9-methyl ester, which showed stronger activity against Gram-positive bacteria than Gram-negative bacteria [36]. Similarly, compounds isolated from *X. psidii* KT30 demonstrated pronounced activity against Gram-positive strains [37], supporting the observed trend in *X. thienhirunae* SWUF17-44.1. Antifungal activity was also evident, with MICs of 6.25 μg/μL against *C. albicans* and *C. tropicalis*, comparable to the antifungal properties of *Xylaria* spp., which produces piliformic acid and cytochalasin D with MICs of 2.92 and 2.46 μmol/mL against plant pathogen *Colletotrichum gloeosporioides*, respectively [38]. These results suggest that *X. thienhirunae* SWUF17-44.1, like other members of the genus, synthesizes phenolic or polyketide-derived metabolites with significant antimicrobial potential. In addition to antimicrobial activity, the extract exhibited notable antioxidant properties, as confirmed by both DPPH and ABTS assays. Although less potent than the synthetic standard Trolox, the observed activities indicate substantial radical scavenging potential. These findings are consistent with antioxidant activities reported from other *Xylaria* species. For example, the endophytic *Xylaria* sp. KET18 extract displayed 78.3 ± 2.9% inhibition at 600 μg/μL in the DPPH assay [39], while xylarglycosides A and B isolated from *Xylaria* sp. KYJ-15 exhibited IC_{50} values of 9.2 ± 0.03 and 13.3 ± 0.01 μmol/L, respectively [40]. The relatively high total phenolic content of *X. thienhirunae* SWUF17-44.1 suggests that phenolic compounds are key contributors to its antioxidant activity, supporting previous reports linking phenolic enrichment in *Xylaria* extracts with enhanced radical-scavenging efficacy. The extract also showed moderate anti-inflammatory activity, with nitric oxide inhibition (16.737 ± 2.479% at 12.8 μg/mL), suggesting suppression of pro-inflammatory mediator release. This observation is consistent with previous reports on *Xylaria* species. For instance, *Xylaria* sp. SWUF09-62 yielded the novel compounds 6-ethyl-7,8-dihydroxy-4H-chromen-4-one and (3S)-3,4-dihydro-5,7,8-trihydroxy-3-methylisocoumarin, which demonstrated significant NO inhibition in LPS-stimulated RAW264.7 cells, with IC_{50} values of 1.57 ± 0.25 and 3.02 ± 0.27 μg/mL, respectively [41]. Similarly, *X. nigripes* mycelial extract effectively reduced inflammatory mediators, including NO, TNF-α, and IL-6, as well as COX-2

enzyme activity [6]. The combined antioxidant and anti-inflammatory effects of *X. thienhirunae* SWUF17-44.1 metabolites may therefore act synergistically, as oxidative stress and inflammation are interconnected pathways that exacerbate microbial infections.

LC-MS analysis was employed to obtain a detailed metabolite profile of the extract. The TIC revealed 17 distinct peaks, indicating a chemically diverse mixture. Putative annotation based on database matching suggested the presence of several known bioactive molecules, including *p*-acetamidophenol, kolanone, netilmicin, istamycin C1, westiellamide, and 2-(4-Methyl-5-thiazolyl)ethylbutanoate. These compounds are associated with diverse pharmacological functions such as analgesic, antimicrobial, cytotoxic, and surfactant activities [29,31,33,34], suggesting that *X. thienhirunae* SWUF17-44.1 may biosynthesize metabolites with multiple biological effects. The presence of aminoglycosides (netilmicin and istamycin C1) is particularly noteworthy, as these compounds are potent antibacterial agents [42], while westiellamide and kolanone have been reported from cyanobacteria and plants, respectively, and are linked to cytotoxicity and antioxidant properties [33,34]. Although database-based LC-MS annotations cannot confirm the biosynthetic origin of individual metabolites, the detection of such compounds underscores the broad biosynthetic potential of *X. thienhirunae* SWUF17-44.1. Comparable LC-MS-based metabolite profiling has been reported in other *Xylaria* species. For instance, *X. chaiyaphumensis* yielded bassianolide, euphyperin B, prednisone, and xylaropyrone, while *X. subintraflava* produced animicin A, 19,20-epoxycytochalasin C, naringin, rottlerin, and tiliroside with strong antioxidant activity [22]. Likewise, *X. curta* and *X. longipes* were shown to synthesize sesquiterpenoids, cytochalasins, and benzophenones with antimicrobial and cytotoxic activities [43]. In comparison, *X. thienhirunae* SWUF17-44.1 is distinctive in producing netilmicin and istamycin C1 in addition to phenolic derivatives, a combination not previously reported in the genus [2]. This finding underscores the unique biosynthetic potential of *X. thienhirunae* SWUF17-44.1 and broadens the known chemical diversity within *Xylaria*. Chromatographic isolation and purification subsequently yielded four pure compounds, including two known metabolites—4-(2,3-dihydroxypropoxy)benzoic acid and 4-prenyloxybenzoic acid—and two previously undescribed compounds, xylerithienol and xylerithiether. The identification of both novel and known phenolic derivatives reflects the capacity of *X. thienhirunae* SWUF17-44.1 to generate structurally diverse secondary metabolites, a feature characteristic of the genus *Xylaria*. The discovery of xylerithienol and xylerithiether expands the chemical diversity reported from *Xylaria* and provides new structural scaffolds for antimicrobial and antioxidant drug discovery.

The molecular docking results provided mechanistic insights into the antimicrobial activity of the metabolites isolated from *X. thienhirunae* SWUF17-44.1. Several compounds, particularly xylerithiether, 4-(2,3-dihydroxypropoxy)benzoic acid and xylerithienol, exhibited strong predicted binding affinities toward essential bacterial targets, suggesting interference with key metabolic pathways. In Gram-positive bacteria, muramyl ligases E (Mur E), a critical enzyme in peptidoglycan biosynthesis [11], was strongly targeted by xylerithiether, which achieved docking scores higher than the reference β-lactam antibiotics ampicillin and carbenicillin. This suggests a potential mechanism of action through inhibition of early-stage cell-wall precursor biosynthesis. Xylerithienol and 4-(2,3-dihydroxypropoxy)benzoic acid also demonstrated favourable binding affinities, whereas 4-prenyloxybenzoic acid showed comparatively weaker interactions. By contrast, lower binding scores were observed for MurE and combined MurD/MurE targets from Gram-negative bacteria, possibly reflecting structural differences in these enzymes. Nevertheless, muramyl ligases are increasing recognized as promising new targets for antibiotic discovery, particularly for addressing resistance to β-lactam antibiotics [11]. Another important target was dihydropteroate synthase (DHPS), a key enzyme in folate biosynthesis and the classical

target of sulfonamides. Most *X. thienhirunae* SWUF17-44.1 metabolites achieved higher docking scores than the reference drugs, suggesting potential interference with folate-dependent nucleotide biosynthesis and consequent inhibition of bacterial growth [12]. The only exception was 4-prenyloxybenzoic acid, which exhibited relatively moderate binding affinity. As DHPS inhibition blocks tetrahydrofolate production, an essential cofactor for DNA synthesis, this pathway remains a validated and clinically relevant antibacterial target. Comparable DHPS-inhibitory activities have also been reported for metabolites from the endophytic fungus *Paraconiothyrium brasiliense* [44], particularly polyketide- and phenolic-derived compounds, further supporting the potential of *X. thienhirunae* SWUF17-44.1 metabolites as natural antifolate leads. Additional docking analyses indicated that xylerithiether strongly interacted with DNA gyrase B and topoisomerase IV, enzymes essential for bacterial DNA replication and repair. Notably, xylerithiether exhibited stronger predicted affinity for DNA gyrase B than norfloxacin, a clinically used fluoroquinolone, and showed the highest binding score against topoisomerase IV. Most natural compounds that inhibited bacterial DNA gyrase have been studied in plants, only a few studies from fungi, including the fungus *Diaporthe perseae* [45]. In addition, xylerithiether showed strong binding affinity for β-ketoacyl-acyl carrier protein synthase III (FabH), exceeding that of isoniazid, a reference inhibitor of mycolic acid biosynthesis. FabH is an attractive antibacterial target because it is unique to bacteria and plays a key role in the synthesis of essential fatty acids that serve as precursors for membrane lipid formation [15].

Despite these favourable in silico predictions, the purified compounds exhibited higher MIC values than ampicillin in vitro. This discrepancy likely reflects fundamental differences between target-level binding affinity and whole-cell antibacterial efficacy. Ampicillin inhibits penicillin-binding proteins at the terminal stage of peptidoglycan cross-linking and benefits from optimized cellular uptake and rapid bactericidal action, whereas the compounds identified here target early intracellular pathways such as MurE- and DHPS-mediated biosynthesis [12]. The antibacterial activity observed, predominantly against Gram-positive bacteria, particularly for xylerithiether, 4-(2,3-dihydroxypropoxy)benzoic acid, and xylerithienol, is consistent with the higher docking scores obtained for Gram-positive MurE and DHPS compared with their Gram-negative counterparts. Although the MIC values of the purified compounds were higher than those of ampicillin, their distinct modes of action suggest potential utility against β-lactam-resistant strains. Collectively, these findings support a multitarget antibacterial model involving disruption of peptidoglycan precursor formation, folate metabolism, DNA replication, and cell wall lipid biosynthesis, underscoring the promise of *X. thienhirunae* SWUF17-44.1 metabolites as lead structures for further optimization.

The compounds also displayed strong predicted interactions with fungal targets. Against sterol 14-α-demethylase (SDM), a key enzyme in ergosterol biosynthesis [16], xylerithiether achieved a docking score higher than that of fluconazole, while xylerithienol and 4-(2,3-dihydroxypropoxy)benzoic acid also surpassed the reference drug. Targeting fungal SDM remains a widely employed antifungal strategy, as the majority of approved drugs against this enzyme are azole derivatives [46]. Secreted aspartic proteinase-5 (SAP5) is a secreted virulence-associated enzyme that facilitates fungal invasion of host tissues and contributes to enhanced pathogenicity, making it an attractive antifungal drug target [17]. Docking analysis revealed that metabolites from *X. thienhirunae* SWUF17-44.1 exhibited strong binding to SAP5, suggesting their potential to disrupt fungal tissue invasion and biofilm formation. Given the established role of SAP5 in *C. albicans* virulence, selective inhibition of this enzyme could attenuate pathogenicity while offering an alternative to conventional antifungal agents [47]. Another important target is the chitin biosynthesis pathway, specifically UDP-N-acetylglucosamine pyrophosphorylase (UAP1). All four

compounds demonstrated binding affinity for this enzyme, suggesting potential disruption of fungal cell wall formation. Since chitin is an essential structural component unique to fungal cell walls and absent in mammalian cells, inhibition of UAP1 catalytic enzyme could provide a selective antifungal strategy with reduced host toxicity [18]. Collectively, these findings highlight the multi-target potential of the newly identified compounds, particularly xylerithiether and xylerithienol, which in several cases exhibited stronger predicted binding than clinically used antibiotics and antifungals. The ability to target multiple bacterial and fungal enzymes suggests a broad-spectrum mode of action and supports the pharmacological relevance of *X. thienhirunae* SWUF17-44.1 metabolites as promising scaffolds for the development of new antimicrobial agents.

5. Conclusions

This study reports the discovery of two novel secondary metabolites, xylerithienol and xylerithiether, isolated for the first time from *X. thienhirunae* SWUF17-44.1. These compounds were structurally elucidated using 1D and 2D NMR techniques and mass spectrometry and represent new additions to the diverse chemical repertoire of the genus *Xylaria*. Molecular docking analyses revealed that xylerithiether exhibited strong binding affinities to bacterial muramyl ligase E, DNA gyrase, and fungal sterol 14-α-demethylase, often surpassing standard antibiotics and antifungals. Xylerithienol also demonstrated potent interactions with topoisomerases and fungal proteinases, supporting its role as a promising antimicrobial agent. Alongside these novel metabolites, the extract contained known bioactive compounds such as 4-(2,3-dihydroxypropoxy)benzoic acid and 4-prenyloxybenzoic acid, which contributed antioxidant and anti-inflammatory effects. The combined presence of novel and known metabolites underscores *X. thienhirunae* as a valuable source of structurally diverse bioactive natural products and highlights its potential for future drug discovery and biotechnological applications.

Supplementary Materials: The following supporting information can be downloaded at: https://www.mdpi.com/article/10.3390/jof12020093/s1. Table S1: Details of the targeted proteins used in this study, including their PDB codes and originating organisms; Figure S1: Standard curve of gallic acid; Figure S2: Total ion chromatogram (TIC) profile operated from negative mode; Table S2: Mass spectra data of separated and predicted peaks from *X. thienhirunae* SWUF17-44.1 in negative mode; Figure S3: The chromatograms from preparative-HPLC of crude extracts and selected peaks are presented for structure elucidation; Table S3: The ^{1}H (600 MHz, CD_3OD), ^{13}C (150 MHz, CD_3OD) NMR and their correlation data of *X. thienhirunae* SWUF17-44.1; Figure S4: NMR spectra of xylerithienol recorded in methanol-d_4 (CD_3OD) at 600 MHz: (A) ^{1}H NMR, (B) ^{13}C DEPTQ, (C) ^{1}H-^{1}H COSY, (D) HSQC, and (E) HMBC; Figure S5: NMR spectra of xylerithiether recorded in methanol-d_4 (CD_3OD) at 600 MHz: (A) ^{1}H NMR, (B) ^{13}C DEPTQ, (C) ^{1}H-^{1}H COSY, (D) HSQC, and (E) HMBC; Figure S6: NMR spectra of 4-(2,3-dihydroxypropoxy)benzoic acid recorded in methanol-d_4 (CD_3OD) at 600 MHz: (A) ^{1}H NMR, (B) ^{13}C DEPTQ, (C) ^{1}H-^{1}H COSY, (D) HSQC, and (E) HMBC; Figure S7: NMR spectra of 4-prenyloxybenzoic acid recorded in methanol-d_4 (CD_3OD) at 600 MHz: (A) ^{1}H NMR, (B) ^{13}C DEPTQ, (C) ^{1}H-^{1}H COSY, (D) HSQC, and (E) HMBC; Figure S8: Molecular docking visualization of xylerithiether with representative antibacterial target proteins based on GoldScore results; Figure S9: Molecular docking visualization of xylerithienol with representative antibacterial target proteins based on GoldScore results; Figure S10: Molecular docking visualization of 4-(2,3-dihydroxypropoxy)benzoic acid with representative antibacterial target proteins based on GoldScore results; Figure S11: Molecular docking visualization of 4-(2,3-dihydroxypropoxy)benzoic acid with representative antifungal target proteins based on GoldScore results; Figure S12: Molecular docking visualization of 4-prenyloxybenzoic acid with representative antibacterial target proteins based on GoldScore results; Figure S13: Molecular docking visualization of 4-prenyloxybenzoic acid with

representative antifungal target proteins based on GoldScore results; Table S4: The separation of fractions, the retention and the quantity of *X. thienhirunae* SWUF17-44.1 in mg.

Author Contributions: Conceptualization, C.P. and N.S.; methodology, P.T., P.K. and N.S.; software, L.N., S.D.S. and K.C.; validation, L.N., S.D.S., K.C., C.P. and N.S.; formal analysis, P.T. and P.K.; investigation, P.T.; resources, C.P. and N.S.; data curation, N.S.; writing—original draft preparation, P.T. and N.S.; writing—review and editing, L.N., S.D.S., K.C. and C.P.; visualization, P.T. and N.S.; supervision, N.S.; funding acquisition, P.T. and N.S. All authors have read and agreed to the published version of the manuscript.

Funding: This research project is supported by National Research Council of Thailand (NRCT): (Contact No. N41A640345), the European Regional Development Fund—Project ENOCH (No. CZ.02.1.01/0.0/0.0/16_019/0000868), and the Czech Agency Grant—Project 23-05474S.

Institutional Review Board Statement: Not applicable.

Informed Consent Statement: Not applicable.

Data Availability Statement: The original contributions presented in this study are included in the article/Supplementary Material. Further inquiries can be directed to the corresponding author.

Acknowledgments: P.T., P.K. and N.S. thank Wanlaya Tanechpongtamb for her valuable suggestions on the molecular docking analysis of antimicrobial activities.

Conflicts of Interest: The authors declare no conflicts of interest.

Abbreviations

The following abbreviations are used in this manuscript:

CYP51	Sterol 14-α-demethylase
DHPS	Dihydropteroate synthase
FabH	β-ketoacyl-acyl carrier protein synthase III
LC-MS	Liquid chromatography–mass spectrometry
Mur	Muramyl ligase
SAP5	Secreted aspartic proteinase-5
TIC	Total ion chromatogram
TLC	Thin-layer chromatography
UAP1	UDP-N-acetylglucosamine pyrophosphorylase

References

1. Suwannasai, N.; Sangvichien, E.; Phosri, C.; McCloskey, S.; Wangsawat, N.; Thamvithayakorn, P.; Ruchikachorn, N.; Thienhirun, S.; Mekkamol, S.; Sihanonth, P. Exploring the Xylariaceae and its relatives. *Bot. Stud.* **2023**, *64*, 15. [CrossRef]
2. Chen, W.; Yu, M.; Chen, S.; Gong, T.; Xie, L.; Liu, J.; Bian, C.; Huang, G.; Zheng, C. Structures and biological activities of secondary metabolites from *Xylaria* spp. *J. Fungi.* **2024**, *10*, 190. [CrossRef] [PubMed]
3. Kuhnert, E.; Navarro-Muñoz, J.; Becker, K.; Stadler, M.; Collemare, J.; Cox, R. Secondary metabolite biosynthetic diversity in the fungal family Hypoxylaceae and *Xylaria hypoxylon*. *Stud. Mycol.* **2021**, *99*, 100118. [CrossRef] [PubMed]
4. Sresuksai, K.; Sawadsitang, S.; Jantaharn, P.; Noppawan, P.; Churat, A.; Suwannasai, N.; Mongkolthanaruk, W.; Senawong, T.; Tontapha, S.; Moontragoon, P. Antiproliferative polyketides from fungus *Xylaria* cf. *Longipes* SWUF08-81 in different culture media. *Nat. Prod. Bioprospect.* **2024**, *14*, 6. [CrossRef]
5. Liang, A.-L.; Tan, Y.-F.; Lu, W.-Y.; Xu, P.-J.; Yuan, Y.-Y.; Chen, Q.-A.; Long, H.-P.; Wang, W.-X.; Li, J. A comprehensive review of the metabolites, biological activities, and clinical application of a medicinal fungus *Xylaria nigripes*. *J. Ethnopharmacol.* **2025**, *350*, 120041. [CrossRef] [PubMed]
6. Divate, R.D.; Chung, Y.-C. In vitro and in vivo assessment of anti-inflammatory and immunomodulatory activities of *Xylaria nigripes* mycelium. *J. Funct. Foods* **2017**, *35*, 81–89. [CrossRef]
7. Miral, A.; Ferron, S.; Rouaud, I.; Slyambayev, D.; Bousarghin, L.; Camuzet, C.; Belouzard, S.; Séron, K.; Le Pogam, P.; Tranchimand, S. Eremoxylarins D–J, antibacterial eremophilane sesquiterpenes discovered from an endolichenic strain of *Xylaria hypoxylon*. *J. Nat. Prod.* **2023**, *86*, 730–738. [CrossRef]

8. Li, M.; Xiong, J.; Huang, Y.; Wang, L.-J.; Tang, Y.; Yang, G.-X.; Liu, X.-H.; Wei, B.-G.; Fan, H.; Zhao, Y. Xylapyrrosides A and B, two rare sugar-morpholine spiroketal pyrrole-derived alkaloids from *Xylaria nigripes*: Isolation, complete structure elucidation, and total syntheses. *Tetrahedron* **2015**, *71*, 5285–5295. [CrossRef]
9. Zhang, X.; Fan, Y.; Ye, K.; Pan, X.; Ma, X.; Ai, H.; Shi, B.; Liu, J. Six unprecedented cytochalasin derivatives from the potato endophytic fungus *Xylaria curta* E10 and their cytotoxicity. *Pharmaceuticals* **2023**, *16*, 193. [CrossRef]
10. Naddaf, M. 40 million deaths by 2050: Toll of drug-resistant infections to rise by 70%. *Nature* **2024**, *633*, 747–748. [CrossRef]
11. Kouidmi, I.; Levesque, R.C.; Paradis-Bleau, C. The biology of Mur ligases as an antibacterial target. *Mol. Microbiol.* **2014**, *94*, 242–253. [CrossRef]
12. Sanyal, D.; Shivram, A.; Pandey, D.; Banerjee, S.; Uversky, V.N.; Muzata, D.; Chivukula, A.; Jasuja, R.; Chattopadhyay, K.; Chowdhury, S. Mapping dihydropteroate synthase evolvability through identification of a novel evolutionarily critical substructure. *Int. J. Biol. Macromol.* **2025**, *311*, 143325. [CrossRef]
13. Webber, M.A.; Ricci, V.; Whitehead, R.; Patel, M.; Fookes, M.; Ivens, A.; Piddock, L.J. Clinically relevant mutant DNA gyrase alters supercoiling, changes the transcriptome, and confers multidrug resistance. *mBio* **2013**, *4*, e00273. [CrossRef]
14. Kumar, A.; Prasun, C.; Rathi, E.; Nair, M.S.; Kini, S.G. Identification of potential DNA gyrase inhibitors: Virtual screening, extra-precision docking and molecular dynamics simulation study. *Chem. Pap.* **2023**, *77*, 6717–6727. [CrossRef]
15. Verma, S.; Gupta, P.; Lal, S.; Narang, R.; Mujwar, S.; Saini, S.; Sharma, J. Recent Developments of the β-ketoacyl-acyl carrier protein synthase III (FabH) Inhibitors: Emerging Indication as Antibacterial Agents. *Eur. J. Med. Chem.* **2025**, *298*, 117995. [CrossRef] [PubMed]
16. Kelly, S.L.; Lamb, D.C.; Jackson, C.J.; Warrilow, A.G.; Kelly, D.E. The biodiversity of microbial cytochromes P450. *Adv. Microb. Physiol.* **2003**, *47*, 131–186. [CrossRef]
17. Jeevitha, S.; Manikandan, A.; Pavan, P.; Rubalakshmi, G. Anticandidal Effect of New Imidazole Derivatives Over Aspartic Protease Inhibition. *Chem. Biodivers.* **2024**, *21*, e202301276. [CrossRef]
18. Raimi, O.G.; Hurtado-Guerrero, R.; Borodkin, V.; Ferenbach, A.; Urbaniak, M.D.; Ferguson, M.A.; van Aalten, D.M. A mechanism-inspired UDP-N-acetylglucosamine pyrophosphorylase inhibitor. *RSC Chem. Biol.* **2020**, *1*, 13–25. [CrossRef]
19. Emran, T.B.; Rahman, M.A.; Uddin, M.M.N.; Dash, R.; Hossen, M.F.; Mohiuddin, M.; Alam, M.R. Molecular docking and inhibition studies on the interactions of *Bacopa monnieri*'s potent phytochemicals against pathogenic *Staphylococcus aureus*. *DARU J. Pharm. Sci.* **2015**, *23*, 26. [CrossRef] [PubMed]
20. Meng, X.-Y.; Zhang, H.-X.; Mezei, M.; Cui, M. Molecular docking: A powerful approach for structure-based drug discovery. *Curr. Comput. Aided Drug Des.* **2011**, *7*, 146–157. [CrossRef]
21. Wangsawat, N.; Ju, Y.-M.; Phosri, C.; Whalley, A.J.; Suwannasai, N. Twelve new taxa of *Xylaria* associated with termite nests and soil from northeast Thailand. *Biology* **2021**, *10*, 575. [CrossRef]
22. Wangsawat, N.; Nahar, L.; Sarker, S.D.; Phosri, C.; Evans, A.R.; Whalley, A.J.; Choowongkomon, K.; Suwannasai, N. Antioxidant activity and cytotoxicity against cancer cell lines of the extracts from novel *Xylaria* species associated with termite nests and LC-MS analysis. *Antioxidants* **2021**, *10*, 1557. [CrossRef] [PubMed]
23. Sarker, S.D.; Nahar, L.; Kumarasamy, Y. Microtitre plate-based antibacterial assay incorporating resazurin as an indicator of cell growth, and its application in the in vitro antibacterial screening of phytochemicals. *Methods* **2007**, *42*, 321–324. [CrossRef]
24. Gharaghani, M.; Rezaei-Matehkolaei, A.; Mahmoudabadi, A.Z.; Keikhaei, B. The frequency, antifungal susceptibility and enzymatic profiles of *Candida* species isolated from neutropenic patients. *Jundishapur J. Microbiol.* **2016**, *9*, e41446. [CrossRef]
25. Staniszewska, M.; Kuryk, Ł.; Gryciuk, A.; Kawalec, J.; Rogalska, M.; Baran, J.; Łukowska-Chojnacka, E.; Kowalkowska, A. In vitro anti-candida activity and action mode of benzoxazole derivatives. *Molecules* **2021**, *26*, 5008. [CrossRef] [PubMed]
26. Rusu, M.E.; Gheldiu, A.-M.; Mocan, A.; Moldovan, C.; Popa, D.-S.; Tomuta, I.; Vlase, L. Process optimization for improved phenolic compounds recovery from walnut (*Juglans regia* L.) septum: Phytochemical profile and biological activities. *Molecules* **2018**, *23*, 2814. [CrossRef]
27. Karin, B.; Nantavisai, K.; Thamvithayakorn, P.; Chotelersak, K.; Phosri, C.; Suwannasai, N. Evaluation of Biological Activities and Cytotoxicity of *Microporus vernicipes* PW17-173 and *Microporus xanthopus* PP17-16 Mushroom Extracts for Natural Cosmetics Applications. *Sci. Ess. J.* **2024**, *40*, 58–73.
28. Cole, J.; Nissink, J.W.M.; Taylor, R. *Protein-Ligand Docking and Virtual Screening with GOLD*; Taylor & Francis CRC Press: Boca Raton, FL, USA, 2005; pp. 379–415.
29. Hinz, B.; Cheremina, O.; Brune, K. Acetaminophen (paracetamol) is a selective cyclooxygenase-2 inhibitor in man. *FASEB J.* **2008**, *22*, 383–390. [CrossRef]
30. Ahmad, A.; Husain, A.; Khan, S.A.; Mujeeb, M.; Bhandari, A. Synthesis, antimicrobial and antitubercular activities of some novel pyrazoline derivatives. *J. Saudi Chem. Soc.* **2016**, *20*, 577–584. [CrossRef]
31. Ikeda, D.; Horiuchi, Y.; Yoshida, M.; Miyasaka, T.; Kondo, S.; Umezawa, H. Isolation and structures of istamycin components. *Carbohydr. Res.* **1982**, *109*, 33–45. [CrossRef]

32. Miller, G.H.; Arcieri, G.; Weinstein, M.J.; Waitz, J.A. Biological activity of netilmicin, a broad-spectrum semisynthetic aminoglycoside antibiotic. *Antimicrob. Agents Chemother.* **1976**, *10*, 827–836. [CrossRef]
33. Hussain, R.; Owegby, A.; Parimoo, P.; Waterman, P. Kolanone, a novel polyisoprenylated benzophenone with antimicrobial properties from the fruit of *Garcinia kola*. *Planta Med.* **1982**, *44*, 78–81. [CrossRef]
34. Prinsep, M.R.; Moore, R.E.; Levine, I.A.; Patterson, G.M. Westiellamide, a bistratamide-related cyclic peptide from the blue-green alga *Westiellopsis prolifica*. *J. Nat. Prod.* **1992**, *55*, 140–142. [CrossRef]
35. Singh, A.; Malhotra, D.; Singh, K.; Chadha, R.; Bedi, P.M.S. Thiazole derivatives in medicinal chemistry: Recent advancements in synthetic strategies, structure activity relationship and pharmacological outcomes. *J. Mol. Struct.* **2022**, *1266*, 133479. [CrossRef]
36. Rakshith, D.; Gurudatt, D.M.; Rao, H.Y.; Mohana, N.C.; Nuthan, B.; Ramesha, K.; Satish, S. Bioactivity-guided isolation of antimicrobial metabolite from *Xylaria* sp. *Process Biochem.* **2020**, *92*, 378–385. [CrossRef]
37. Indarmawan, T.; Mustopa, A.Z.; Budiarto, B.R.; Tarman, K. Antibacterial activity of extracellular protease isolated from an algicolous fungus *Xylaria psidii* KT30 against gram-positive bacteria. *HAYATI J. Biosci.* **2016**, *23*, 73–78. [CrossRef]
38. Elias, L.M.; Fortkamp, D.; Sartori, S.B.; Ferreira, M.C.; Gomes, L.H.; Azevedo, J.L.; Montoya, Q.V.; Rodrigues, A.; Ferreira, A.G.; Lira, S.P. The potential of compounds isolated from *Xylaria* spp. as antifungal agents against anthracnose. *Braz. J. Microbiol.* **2018**, *49*, 840–847. [CrossRef]
39. Pham, N.S.; Le, T.T.X.; Pham, Q.A.; Vu, T.H.N.; Quach, N.T.; Nguyen, T.T.L.; Do, T.T.; Do, H.A.; Tran, H.Q.; Chu, K.-S. The Cytotoxicity and Antioxidant Potentials of the Endophytic Fungus *Xylaria* sp. KET18 Associated with *Keteleeria evelyniana* Mast. *Appl. Sci.* **2024**, *14*, 11070. [CrossRef]
40. Dong, G.; Chenzhe, L.; Yan, S.; Jiapeng, W.; Chengyao, W.; Li, Z.; Yujun, Y.; Jiaqi, L.; Bijian, H.; Le, C. Steroids and dihydroisocoumarin glycosides from *Xylaria* sp. by the one strain many compounds strategy and their bioactivities. *Chin. J. Nat. Med.* **2023**, *21*, 154–160. [CrossRef] [PubMed]
41. Patjana, T.; Jantaharn, P.; Katrun, P.; Mongkolthanaruk, W.; Suwannasai, N.; Senawong, T.; Tontapha, S.; Amornkitbumrung, V.; McCloskey, S. Anti-inflammatory and cytotoxic agents from *Xylaria* sp. SWUF09-62 fungus. *Nat. Prod. Res.* **2021**, *35*, 2010–2019. [CrossRef]
42. Kong, J.; Wu, Z.-X.; Wei, L.; Chen, Z.-S.; Yoganathan, S. Exploration of antibiotic activity of aminoglycosides, in particular ribostamycin alone and in combination with ethylenediaminetetraacetic acid against pathogenic bacteria. *Front. Microbiol.* **2020**, *11*, 1718. [CrossRef] [PubMed]
43. Wei, S.-S.; Lai, J.-Y.; Chen, C.; Zhang, Y.-J.; Nong, X.-M.; Qiu, K.-D.; Duan, F.-F.; Zou, Z.-X.; Tan, H.-B. Sesquiterpenes and α-pyrones from an endophytic fungus *Xylaria* curta YSJ-5. *Phytochemistry* **2024**, *220*, 114011. [CrossRef] [PubMed]
44. Sathiyaseelan, A.; Saravanakumar, K.; Mariadoss, A.V.A.; Kim, K.M.; Wang, M.-H. Antibacterial activity of ethyl acetate extract of endophytic fungus (*Paraconiothyrium brasiliense*) through targeting dihydropteroate synthase (DHPS). *Process Biochem.* **2021**, *111*, 27–35. [CrossRef]
45. Manzano, J.A.H.; Abanto, J.C.D.; Dayo, B.A.F.; Llames, L.C.J.; Gonzaga, M.G.E.; Brogi, S.; Macabeo, A.P.G. DNA gyrase-inhibitory antimicrobial anthraquinone from the endophytic Sordariomycetes fungus *Diaporthe perseae*. *Arch. Microbiol.* **2025**, *207*, 239. [CrossRef]
46. Leaver, D.J. Synthesis and biological activity of sterol 14α-demethylase and sterol C24-methyltransferase inhibitors. *Molecules* **2018**, *23*, 1753. [CrossRef]
47. Bras, G.; Satala, D.; Juszczak, M.; Kulig, K.; Wronowska, E.; Bednarek, A.; Zawrotniak, M.; Rapala-Kozik, M.; Karkowska-Kuleta, J. Secreted aspartic proteinases: Key factors in *Candida* infections and host-pathogen interactions. *Int. J. Mol. Sci.* **2024**, *25*, 4775. [CrossRef] [PubMed]